Synemin is expressed in reactive astrocytes in neurotrauma and interacts differentially with vimentin and GFAP intermediate filament networks

Runfeng Jing[1,*], Ulrika Wilhelmsson[2,*], William Goodwill[1], Lizhen Li[2], Yihang Pan[1], Milos Pekny[2,‡] and Omar Skalli[1,‡,§]

[1]Department of Cellular Biology and Anatomy and Feist-Weiller Cancer Center, Louisiana State University Health Sciences Center, Shreveport, LA 71130, USA
[2]Center for Brain Repair and Rehabilitation, Department of Clinical Neuroscience and Rehabilitation, Institute of Neuroscience and Physiology, Sahlgrenska Academy, Göteborg University, Medicinaregatan 9A, 41390 Göteborg, Sweden

*These authors contributed equally to this work
‡This work represents a joint effort of the two laboratories
§Author for correspondence (e-mail: oskall@lsuhsc.edu)

Accepted 7 February 2007
Journal of Cell Science 120, 1267-1277 Published by The Company of Biologists 2007
doi:10.1242/jcs.03423

Summary

Immature astrocytes and astrocytoma cells contain synemin and three other intermediate filament (IF) proteins: glial fibrillary acidic protein (GFAP), vimentin and nestin. Here, we show that, after neurotrauma, reactive astrocytes produce synemin and thus propose synemin as a new marker of reactive astrocytes. Comparison of synemin mRNA and protein levels in brain tissues and astrocyte cultures from wild-type, *Vim*$^{-/-}$ and *Gfap*$^{-/-}$*Vim*$^{-/-}$ mice showed that in the absence of vimentin, synemin protein was undetectable although synemin mRNA was present at wild-type levels. By contrast, in *Gfap*$^{-/-}$ astrocytes, synemin protein and mRNA levels, as well as synemin incorporation into vimentin IFs, were unaltered. Biochemical assays with purified proteins suggested that synemin interacts with GFAP IFs like an IF-associated protein rather than like a polymerization partner, whereas the opposite was true for synemin interaction with vimentin. In transfection experiments, synemin did not incorporate into normal, filamentous GFAP networks, but integrated into vimentin and GFAP heteropolymeric networks. Thus, alongside GFAP, vimentin and nestin, reactive astrocytes contain synemin, whose accumulation is suppressed post-transcriptionally in the absence of a polymerization partner. In astrocytes, this partner is vimentin and not GFAP, which implies a functional difference between these two type III IF proteins.

Key words: Astrocytes, Intermediate filament, GFAP, Vimentin

Introduction

Intermediate filament (IF) networks constitute dynamic scaffolds integrating the cytoplasm on a structural and functional level (for reviews, see Chang and Goldman, 2004; Coulombe and Wong, 2004; Lane and Pekny, 2004; Omary et al., 2004). IFs can assemble from approximately 60 proteins that share a short signature sequence and a tripartite domain, whose major structural feature is a central α-helical domain of 310 amino acids (Herrmann and Aebi, 2004). Five types of IF proteins are recognized based on sequence homologies and on the intron-exon organization of the genes.

IF proteins are expressed in a cell-type specific pattern (for reviews, see Omary et al., 2004; Coulombe and Wong, 2004). This pattern is often established after a series of developmentally regulated transitions in IF proteins, and it is often altered in diseases. For example, during development and in pathological situations, astrocytes can simultaneously express two type III [vimentin and glial fibrillary acidic protein (GFAP)] and two type IV (synemin and nestin) IF proteins. Astrocyte precursors contain vimentin, nestin and synemin (Lendahl et al., 1990; Rutka et al., 1997; Sultana et al., 2000). As astrocytes differentiate, these IF proteins are replaced progressively by GFAP. In astrocytoma cells, this process is reversed and the IF protein composition often resembles that of immature astrocytes (Dahlstrand et al., 1992; Jing et al., 2005; Rutka et al., 1997). In neurotrauma and in ischemic and neurodegenerative lesions, reactive astrocytes overexpress GFAP and re-express vimentin and nestin (for reviews, see Eng et al., 2000; Pekny and Pekna, 2004; Pekny and Wilhelmsson, 2006).

Vimentin and GFAP are ~80% homologous at the primary protein sequence level, and each can polymerize on its own or form heteropolymers with the other (Quinlan and Franke, 1983; Wang et al., 1984). Synemin and nestin, however, exhibit only minor sequence homologies with each other and with other IF proteins, and possess a large C-terminal domain that is three to four times larger than that of vimentin or GFAP (Lendahl et al., 1990; Bellin et al., 1999; Titeux et al., 2001). In humans, the synemin gene is alternatively spliced into two isoforms called α and β, with the C-terminal domain of α-synemin containing a 312 amino-acid insertion when compared with β-synemin (Titeux et al., 2001). The C-terminal domain of α-synemin contains binding sites for α-actinin and vinculin (Bellin et al., 1999; Bellin et al., 2001), whereas β-synemin can interact with dystrobrevin (Mizuno et al., 2001). Synemin cannot assemble into IFs on its own but can

copolymerize with vimentin (Bellin et al., 1999; Bilak et al., 1998; Marvin et al., 1998; Sandoval, 1983; Steinert et al., 1999; Titeux et al., 2001), resembling in this respect the type IV IF protein nestin (Eliasson et al., 1999).

Synemin is the least understood of the IF proteins expressed by astrocytes. In this study, we investigated whether reactive astrocytes in neurotrauma express synemin and how the genetic ablation of GFAP and/or vimentin influences this expression. We also analyzed in detail the interactions of synemin with GFAP and vimentin. These studies provide novel information on the IF protein composition of reactive astrocytes and identify synemin as a novel marker of reactive astrocytes. Our results also show that, in astrocytes, synemin accumulation into GFAP-containing IFs is dependent on vimentin expression, suggesting that vimentin may function as an adaptor for synemin incorporation into GFAP-containing IFs.

Results

Synemin immunoreactivity in reactive astrocytes in adult wild-type and *Gfap*$^{-/-}$*Vim*$^{-/-}$ mice

To assess the expression of synemin in reactive astrocytes in neurotrauma, we subjected adult wild-type and *Gfap*$^{-/-}$*Vim*$^{-/-}$ mice to unilateral entorhinal cortex lesioning. In this injury model, the perforant pathway is interrupted, triggering astrocyte activation in the denervated outer molecular layer of the dentate gyrus of the hippocampus. In wild-type mice, GFAP immunoreactivity increased and synemin immunoreactivity was detected in the outer molecular layer on the injured side 4 days (Fig. 1A-B) and 14 days (data not shown) after lesioning. No synemin immunoreactivity was seen on the uninjured site (data not shown), which is in agreement with recent findings showing that α- and β-synemin are not present in the dentate gyrus of normal, adult mice (Izmiryan et al., 2006). Synemin and GFAP immunoreactivity colocalized in reactive astrocytes both in the denervated dentate gyrus (Fig. 1C-E) and in the lesioned entorhinal cortex (data not shown). In *Gfap*$^{-/-}$*Vim*$^{-/-}$ mice, however, the only detectable synemin immunoreactivity was that associated with blood vessels as determined by double immunofluorescence with synemin and α-smooth muscle actin antibodies (Fig. 1H-J).

Synemin protein but not mRNA is reduced in the brains of *Gfap*$^{-/-}$*Vim*$^{-/-}$ neonatal mice

Next, we analyzed synemin expression in the cerebral hemispheres of 2-day-old wild-type and *Gfap*$^{-/-}$*Vim*$^{-/-}$ mice. Western blot analysis of total protein extracts from wild-type mice revealed bands of 210 and 170 kDa, corresponding to α- and β-synemin, respectively (Fig. 2A); α-synemin was more abundant than β-synemin. By contrast, α-synemin was barely detectable in cerebral extracts from *Gfap*$^{-/-}$*Vim*$^{-/-}$ mice, and β-synemin was undetectable. α-synemin protein levels were approximately 95% lower in *Gfap*$^{-/-}$*Vim*$^{-/-}$ mice (P<0.001, n=4 mice/group), as shown by densitometry. Actin levels were comparable in the two groups, indicating equal protein loading. As expected, GFAP and vimentin were abundant in the brain of wild-type mice, but absent in *Gfap*$^{-/-}$*Vim*$^{-/-}$ mice (Fig. 2A).

In reverse transcription PCR (RT-PCR) reactions, fragments of 3.7 and 2.8 kb, corresponding to α- and β-synemin mRNA, respectively, were amplified at similar levels from cerebral tissues of 2-day-old wild-type and *Gfap*$^{-/-}$*Vim*$^{-/-}$ mice (Fig. 2B). The α/β synemin mRNA ratio appears to be higher than the α/β synemin protein ratio seen on western blots. RT-PCR, however, may not provide accurate representation of the α/β synemin mRNA ratio within one sample. This is because the set of primers used is very likely to amplify more efficiently the β-synemin cDNA fragment than the 1 kb-longer α-synemin fragment.

Quantitative RT-PCR assays, performed using conditions under which GAPDH and synemin were amplified with similar efficiencies (data not shown), revealed no difference in cerebral synemin mRNA levels between wild-type and *Gfap*$^{-/-}$*Vim*$^{-/-}$ mice (Fig. 2C).

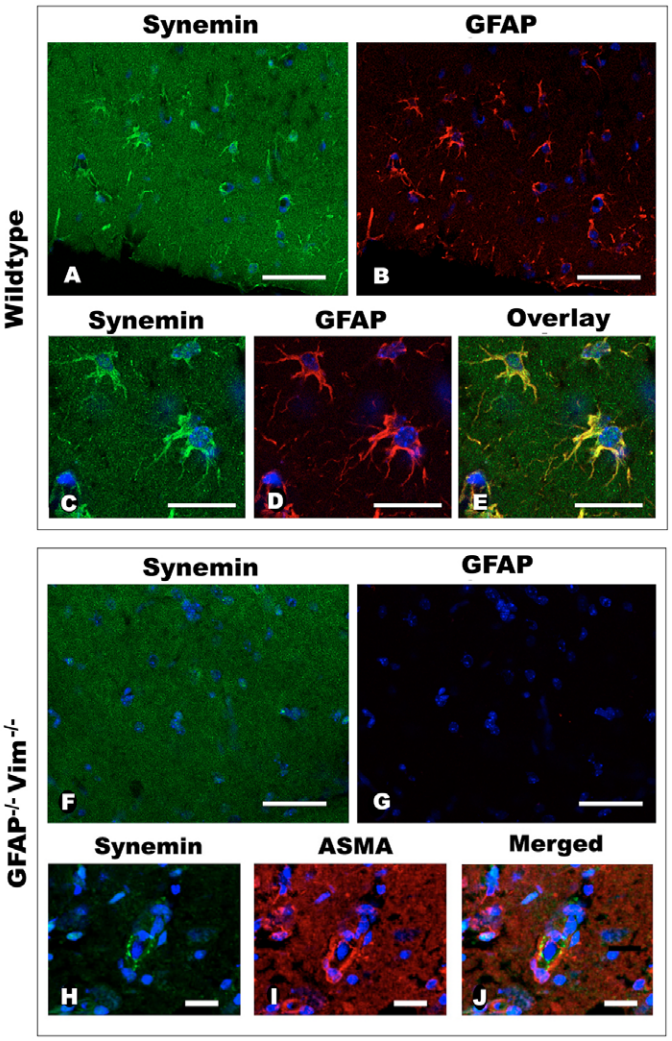

Fig. 1. Double immunofluorescence staining with anti-synemin (A,C,F,H) and anti-GFAP (B,D,G) of the molecular layer of the dentate gyrus 4 days after entorhinal cortex lesion. Nuclei are stained blue with TOPRO-3. In wild-type mice (A-E), low-magnification images (A,B) show strong synemin and GFAP staining in numerous large cells in the dentate gyrus; at high magnification (C-E) these cells appear to be reactive astrocytes. An overlay image (E) shows colocalization (yellow) of synemin and GFAP. In *Gfap*$^{-/-}$*Vim*$^{-/-}$ mice (F-J), reactive astrocytes were negative for synemin and GFAP (F,G). Some perivascular cells, however, were positive for synemin (H,J); these were also positive for α-smooth muscle actin (ASMA) (I,J). Bars, 50 μm (A,B,F,G); 25 μm (C-E,H-J).

Synemin protein does not accumulate in *Vim*$^{-/-}$ astrocytes

Next, we performed a series of experiments with primary (data not shown) and passage 1 astrocytes from 2-day-old wild-type, *Gfap*$^{-/-}$*Vim*$^{-/-}$, *Gfap*$^{-/-}$ and *Vim*$^{-/-}$ mice. RT-PCR showed no qualitative differences in synemin isoforms mRNA levels in cultured astrocytes of all four genotypes (Fig. 3A). Quantitative RT-PCR demonstrated no differences in synemin mRNA levels (Fig. 3B).

By contrast, western blotting analysis revealed that synemin is undetectable in the absence of vimentin, even if GFAP is present, and that synemin is present at levels comparable to wild type in astrocytes expressing vimentin, but not GFAP (Fig. 3C). Western blots also demonstrated that in both wild-type and *Gfap*$^{-/-}$ astrocyte cultures, vimentin and synemin were recovered almost entirely in the cytoskeletal fraction (Fig. 3D), implying that the lack of GFAP does not affect the polymerization state of synemin and vimentin. In wild-type cultures, a pool of approximately 10% of total GFAP was present in the cytosolic fraction (Fig. 3D).

Synemin subcellular distribution in astrocyte cultures

Wild-type astrocyte cultures displayed heterogeneity with respect to synemin expression, and synemin was present in some GFAP-positive and in some GFAP-negative cells. In both GFAP-positive and negative cells and in *Gfap*$^{-/-}$ cultures, synemin was distributed throughout the IF network, from the dense meshwork encircling the nucleus (Fig. 4A) to the dispersed fibers present at the cell periphery (Fig. 4B). The intensity of the synemin immunoreactivity varied along fibers (Fig. 4B).

Synemin has the capacity to interact with vinculin and α-actinin, and in some cell types it colocalizes with these proteins (Bellin et al., 1999; Bellin et al., 2001; Jing et al., 2005; Uyama et al., 2006). In cultured wild-type astrocytes, there was no apparent overlap between the distribution of synemin and vinculin (Fig. 5) or of synemin and α-actinin (data not shown). In *Gfap*$^{-/-}$*Vim*$^{-/-}$ astrocytes, the subcellular distribution of vinculin (Fig. 5C,D) and α-actinin (data not shown) was similar to that observed in wild-type astrocytes (Fig. 5A,B).

Synemin binds equally well to unpolymerized GFAP and vimentin

Our finding that synemin protein is stable in *Gfap*$^{-/-}$, but not in *Gfap*$^{-/-}$*Vim*$^{-/-}$ or *Vim*$^{-/-}$ astrocytes raised the question of whether synemin can interact with GFAP like it does with vimentin. To address this, we performed a series of biochemical assays and transfection experiments.

Bacterially expressed human GFAP, vimentin and α- and β-synemin for biochemical assays were purified to homogeneity by repeated polymerization/depolymerization cycles and gel filtration (Fig. 6A). For overlay assays, GFAP and vimentin were loaded onto SDS-polyacrylamide gels and transferred to nitrocellulose filters, which were overlaid with α-synemin. Binding to the immobilized proteins was assessed with anti-synemin. Synemin bound equally well to GFAP and vimentin, but did not bind to actin (Fig. 6B). Similar results were obtained with β-synemin (data not shown). In the absence of synemin, no signal was detected. These findings are similar to those of Hirako et al. with GFAP and vimentin from bovine optic nerve and with synemin from rabbit stomach smooth muscle (Hirako et al., 2003).

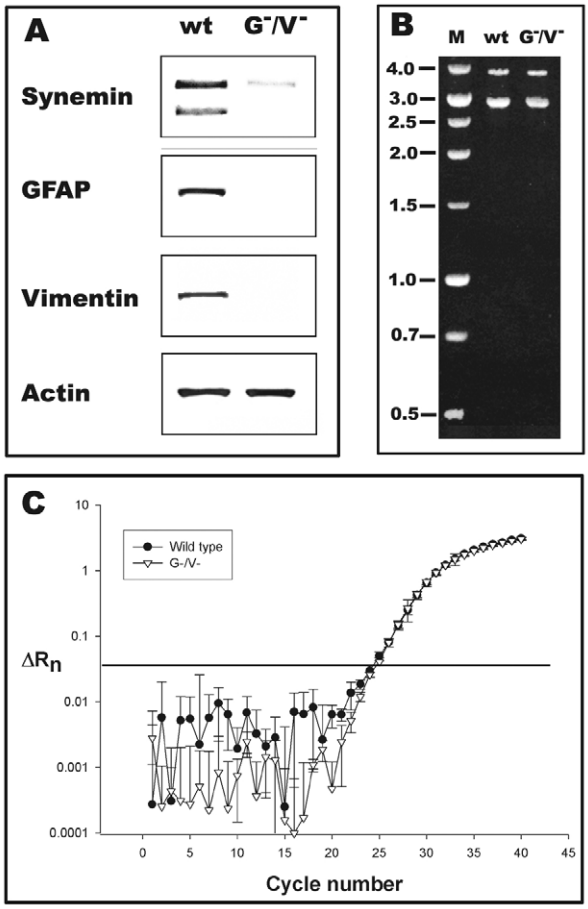

Fig. 2. Synemin expression levels in the cerebral hemisphere of 2-day-old wild-type (wt) and *Gfap*$^{-/-}$*Vim*$^{-/-}$ (G–/V–) mice. (A) Western blots show that synemin protein levels are markedly lower in G–/V– than wild-type mice (upper band, α-synemin; lower band, β-synemin) and confirm the absence of GFAP and vimentin in G–/V– mice. Actin control blots demonstrate equal protein loading. (B) A 0.8% ethidium-bromide agarose gel loaded with RT-PCR products obtained after amplification with synemin primers shows two bands corresponding to α- and β-synemin mRNA in wild-type and G–/V– mice. Lane M shows molecular mass markers, numbers indicate kb. (C) TaqMan real-time PCR amplification curves show no difference in synemin mRNA levels between wild-type mice (circles) and G–/V– mice (triangles). ΔRn, log fluorescence emission intensity of the reporter dye normalized to that of a passive reference dye. Values are mean ± s.e.m. of four different samples. Horizontal line indicates background fluorescence level.

To examine binding under nondenaturing conditions, we performed dot-blot assays. Synemin, GFAP, vimentin and actin were dialyzed against 2 mM Tris-Cl (pH 7.2) and 0.5 mM dithiothreitol (DTT), and various amounts of GFAP, vimentin and actin were adsorbed onto nitrocellulose filters. Under these low-salt, neutral-pH buffer conditions, GFAP and vimentin remain unpolymerized (Kooijman et al., 1995). α-synemin bound to GFAP and vimentin equally well and in proportion to the amount of protein immobilized on the filter, but did not bind to actin (Fig. 6C). Similar results were obtained with β-synemin (data not shown). No signal was detected in the absence of synemin (data not shown).

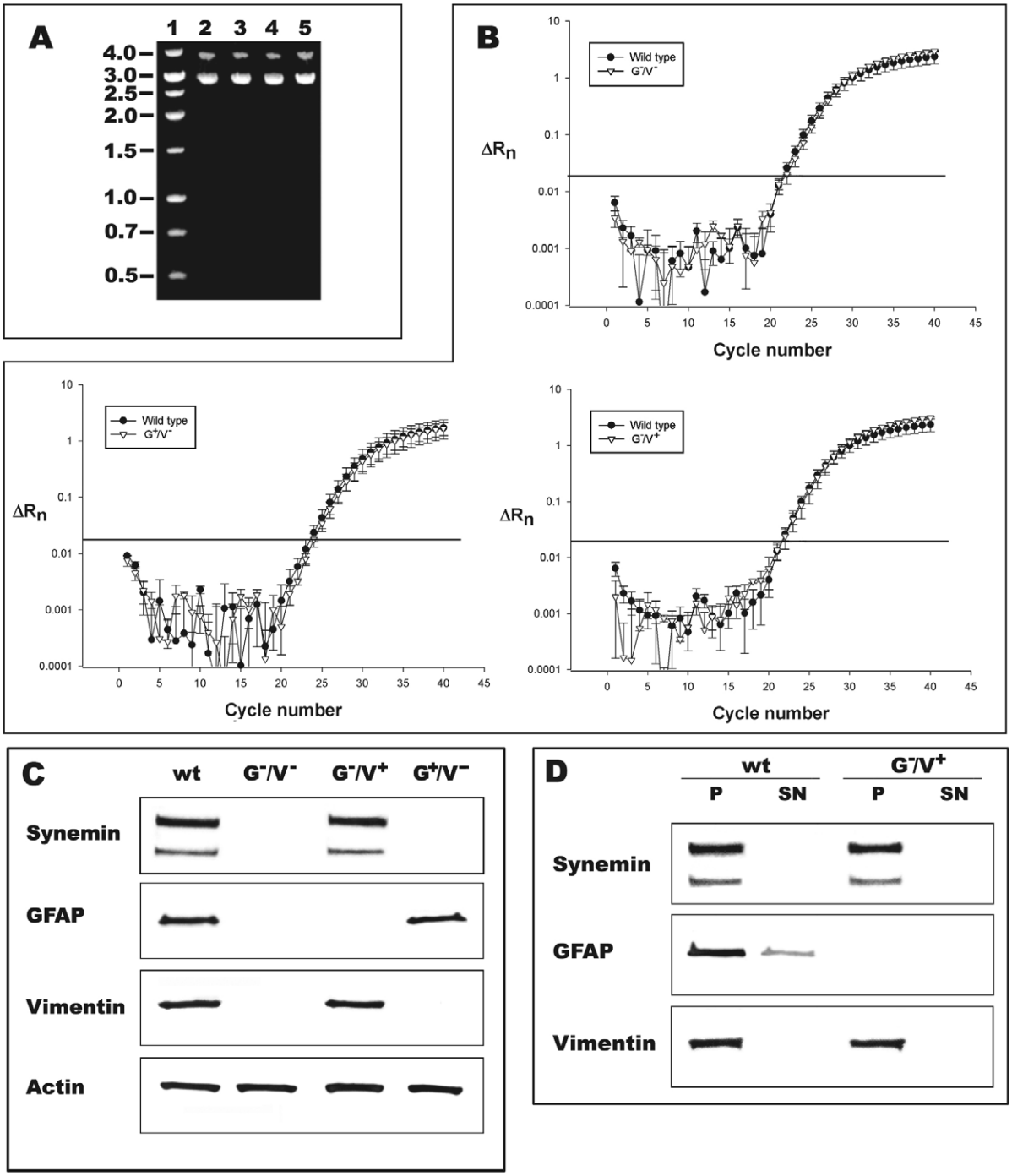

Fig. 3. Synemin mRNA and protein levels in passage 1 astrocyte cultures from the brain of 2-day-old wild-type, *Gfap*$^{-/-}$, *Vim*$^{-/-}$ and *Gfap*$^{-/-}$*Vim*$^{-/-}$ mice. (A) RT-PCR synemin products from wild type (wt) (lane 2), *Gfap*$^{-/-}$*Vim*$^{-/-}$ (G–/V–) (lane 3), *Gfap*$^{-/-}$ (G–/V+) (lane 4) and *Vim*$^{-/-}$ (G+/V–) mice (lane 5). In all genotypes, PCR amplified two bands corresponding to α- and β-synemin mRNA. Lane 1 shows molecular mass markers; numbers to the left indicate size in kb. (B) TaqMan real-time PCR amplification curves show no difference in synemin mRNA levels between wild type (full circles) and the different knockout genotypes (triangles). ΔRn, log fluorescence emission intensity of the reporter dye normalized to a passive reference dye. Values are mean ± s.e.m., *n*=4. Horizontal lines indicate a background fluorescence level. (C) Immunoblots showing synemin, GFAP, vimentin and actin protein levels in passage 1 astrocyte cultures. Synemin was present in astrocytes expressing vimentin, but was undetectable in the absence of vimentin, even when GFAP was present. Actin control blots demonstrate equal protein loading. (D) Immunoblots showing the distribution of synemin, GFAP and vimentin in the detergent-insoluble cytoskeletal fraction (P) and the cytosolic fraction (SN).

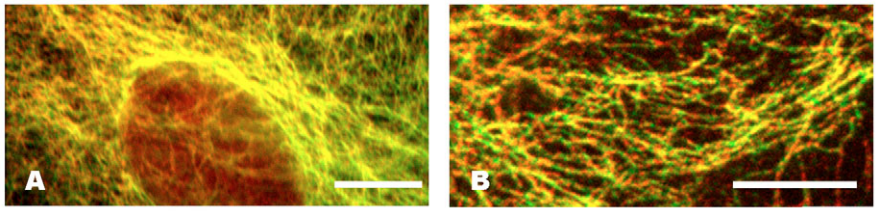

Fig. 4. Superimposed immunofluorescence images of cultured wild-type astrocytes stained with anti-synemin (red) and anti-GFAP (green); in yellow or orange are areas where synemin and GFAP colocalize. Note that these cells also contain vimentin. A and B show that synemin colocalizes with IF in perinuclear (A), intermediate and peripheral cellular regions (B). In the latter, color variations occurring within individual fibers indicate variable ratio of vimentin and synemin. Bars, 5 μm (A); 0.5 μm (B).

In vitro, synemin interacts differently with GFAP and vimentin IFs

To examine whether synemin copolymerizes with GFAP, we mixed α-synemin with GFAP (1:100 molar ratio) in 8 M urea buffer, dialyzed the mixture against a buffer of physiological ionic strength and pH to assemble IFs, subjected it to ultracentrifugation, and analyzed the pellet and supernatant by SDS-PAGE (Fig. 7A). Similar experiments were performed with vimentin, which was used as a positive control because synemin is known to copolymerize with vimentin (Bellin et al., 1999; Titeux et al., 2001). In the presence of GFAP or vimentin, α-synemin was largely recovered in the pellet. However, when α-synemin alone was subjected to this analysis, it was mostly recovered in the supernatant. Similar results were obtained with β-synemin (data not shown). Electron microscopy showed that vimentin and GFAP were capable of polymerizing into IFs (data not shown).

These results do not rule out the possibility that synemin cosediments with GFAP because it binds to GFAP IFs rather than copolymerizes with GFAP. This possibility was examined by mixing α-synemin with GFAP or vimentin IFs assembled in the absence of synemin (preformed IFs). Before addition of preformed IFs, α-synemin was dialyzed against IF assembly buffer and ultracentrifuged to remove insoluble aggregates. When this supernatant was ultracentrifuged a second time, most of the synemin was recovered in the new supernatant (Fig. 7B). Similarly, after incubation with preformed vimentin IFs, most of the α-synemin was recovered in the supernatant. However, after incubation with preformed GFAP IFs, most of the α-synemin was recovered in the pellet (Fig. 7B). Similar results were obtained with β-synemin (data not shown). This suggests that, in vitro, synemin interacts with GFAP IF like an associated protein rather than like a polymerization partner.

GFAP networks have a limited capacity to interact with synemin

To examine the capacity of synemin to associate with GFAP networks in vivo, we performed transfection experiments in SW13-cl2 adrenocortical carcinoma cells. These cells are devoid of cytoplasmic IFs and have been used extensively to study IF protein polymerization (Sarria et al., 1990). Transfection with GFAP cDNA yielded a filamentous GFAP network throughout the cytoplasm, as reported (Chen and Liem, 1994; Schweitzer et al., 2001). However, in approximately 30% of the transfected cells, part of the network consisted of large, brightly stained cables or coils (Fig. 8A). Approximately 5% of the transfected cells did not assemble a GFAP network; instead, the protein accumulated in short comma- or rod-shaped structures (Fig. 8B). These structures stained very brightly with anti-GFAP, suggesting that their formation results from GFAP overexpression.

When SW13-cl2 cells were transiently transfected with GFAP and either α- or β-synemin cDNA, the subcellular distribution of synemin depended on the nature of the GFAP network (Fig. 8C-H). When the network was filamentous, synemin formed small round structures that did not stain with GFAP antibodies (Fig. 8C-D). When high GFAP expression led to the formation of cables or to the total disruption of the GFAP network into large rhomboidal aggregates, synemin was colocalized with those GFAP-rich structures (Fig. 8G,H). When the peripheral part of the cytoplasm contained a filamentous GFAP network and the perinuclear region displayed GFAP-containing cables or coils, synemin antibodies stained only latter structures, not the filamentous portion of the network (Fig. 8E-F). The inability of synemin to co-distribute with the filamentous portion of a GFAP network contrasts with its known capacity to form an extended filamentous network with vimentin (Bellin et al., 1999; Titeux et al., 2001), a

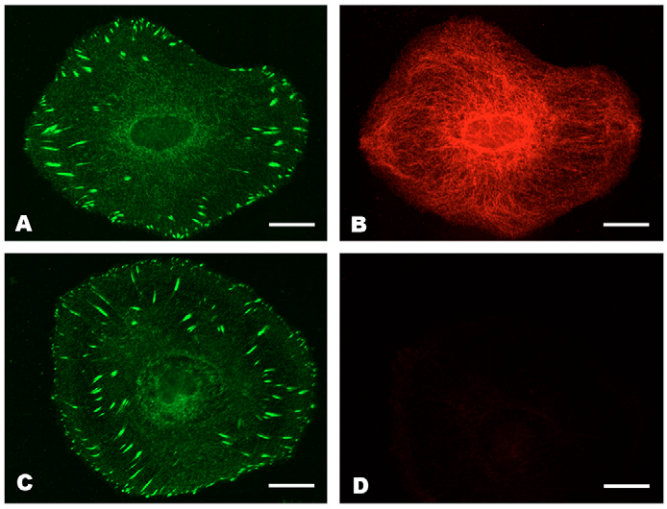

Fig. 5. Double immunofluorescence with anti-vinculin (A,C) and antibodies against α- and β-synemin (B,D) on cultured wild-type astrocytes. In these cells, there is no apparent overlap between vinculin and synemin (A,B). In synemin-positive (A) and synemin-negative cells (C,D), the overall distribution of vinculin (C) is comparable. Bar, 5 μm.

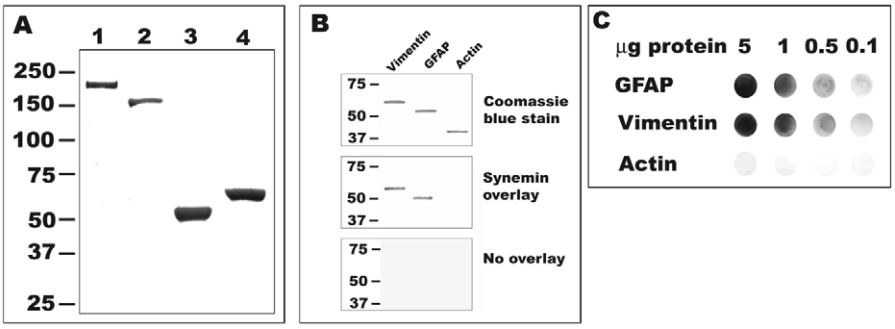

Fig. 6. (A) Coomassie Blue-stained 4-15% SDS-polyacrylamide gel shows bacterially expressed α-synemin (lane 1), β-synemin (lane 2), GFAP (lane 3) and vimentin (lane 4) after purification through polymerization/depolymerization cycles and gel filtration; numbers to the left indicate kDa. (B) Overlay assays to assess binding of α-synemin to vimentin, GFAP and actin. Upper panel: Coomassie Blue-stained gel demonstrates equal protein loading. Middle panel: western blot incubated with α-synemin and then with anti-synemin followed by a secondary antibody. α-synemin bound equally well to monomeric GFAP and vimentin but did not bind to actin. Lower panel: similar western blot incubated with anti-synemin followed by a secondary antibody. (C) Dot-blot assay in which decreasing amounts of GFAP, vimentin and actin were adsorbed to nitrocellulose under nondenaturing, nonpolymerizing conditions. Synemin bound similarly to GFAP and vimentin but did not bind to actin.

capacity that we have also observed in a series of control experiments (data not shown).

Vimentin enables synemin to incorporate into GFAP-containing IF networks

Next, we investigated whether vimentin affects the incorporation of synemin into GFAP networks. SW13-cl2 cell lines were stably transfected with GFAP cDNA (SW13-cl2/G) or vimentin cDNA (SW13-cl2/V). Immunofluorescence staining with anti-GFAP demonstrated a filamentous GFAP network in >95% of SW13-cl2/G cells and little evidence of overexpression. Similarly, anti-vimentin staining showed a filamentous vimentin network in nearly all SW13-cl2/V cells. In SW13-cl2/G cells transiently transfected with vimentin cDNA or in SW13-cl2/V cells transiently transfected with GFAP cDNA, immunofluorescence staining with anti-GFAP and anti-vimentin yielded identical patterns (not shown), consistent with the ability of GFAP and vimentin to coassemble into heteropolymeric networks (Quinlan and Franke, 1983; Wang et al., 1984).

After transient transfection of SW13-cl2/G cells with α- or β-synemin cDNA, synemin failed to incorporate into the GFAP network but instead formed numerous punctate aggregates throughout the cytoplasm (Fig. 9). However, after cotransfection of these cells with vimentin and α- or β-synemin cDNA, synemin was incorporated into the vimentin/GFAP IF network in >90% of the cotransfected cells (Fig. 10A,B). In SW13-cl2/V cells cotransfected with GFAP and α- or β-synemin, synemin and GFAP co-distributed within the same IF network (Fig. 10C-F). Each of the above transfection experiments were performed with three separate SW13-Cl2/G or SW13-cl2/V clones, and each clone yielded similar results.

Discussion

In this study, we demonstrate that reactive astrocytes express synemin in wild-type but not *Gfap*$^{-/-}$*Vim*$^{-/-}$ mice subjected to neurotrauma. Despite normal synemin mRNA levels, synemin failed to accumulate in the brain tissues and astrocyte cultures from newborn *Gfap*$^{-/-}$*Vim*$^{-/-}$ and *Vim*$^{-/-}$ mice, whereas in *Gfap*$^{-/-}$ astrocytes, synemin accumulated normally. Biochemical assays with purified proteins and stable and transient transfection experiments demonstrated that GFAP IF networks have limited capacity to interact with synemin, which contrasts with known synemin ability to interact with vimentin

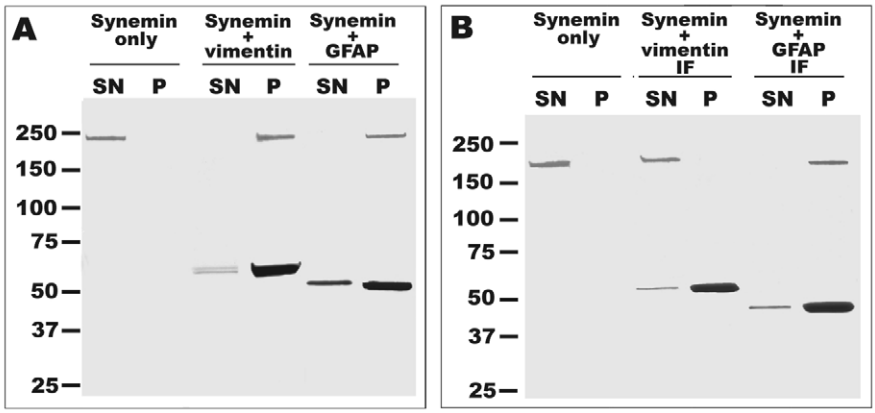

Fig. 7. Coomassie Blue-stained 4-15% SDS-polyacrylamide gels demonstrate changes in synemin sedimentation properties when allowed to copolymerize with vimentin or GFAP (A) or to bind to vimentin or GFAP IFs (B). Numbers indicate molecular mass in kDa. (A) Mixtures of α-synemin and buffer, or of α-synemin and either vimentin or GFAP were assembled in 8 M urea buffer and dialyzed under conditions that promote the assembly of vimentin and GFAP IFs. After dialysis, the mixtures were ultracentrifuged and proteins in the supernatant (SN) and pellet (P) were analyzed by SDS-PAGE. Most α-synemin was recovered in the supernatant in the absence of vimentin or GFAP, but was mostly in the pellet in the presence of these proteins. (B) α-synemin was added either to vimentin or GFAP IFs or to polymerization buffer. After a 1-hour incubation, the mixtures were ultracentrifuged, and proteins in the supernatant (SN) and pellet (P) were analyzed by SDS-PAGE. In the presence of vimentin IFs, α-synemin was mostly recovered in the supernatant. By contrast, in the presence of GFAP IFs, most α-synemin was recovered in the pellet.

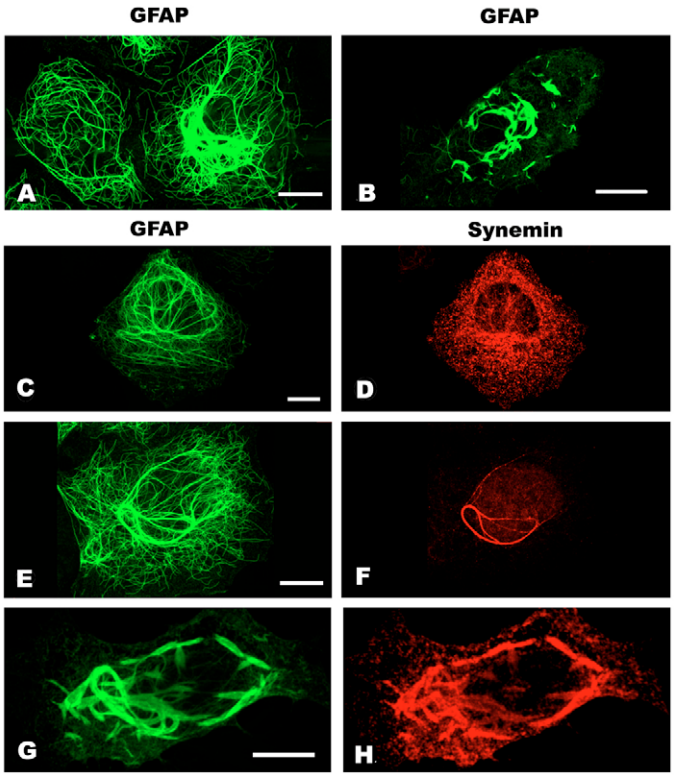

Fig. 8. SW13-cl2 cells transiently transfected with GFAP (A,B) and cotransfected with GFAP and α-synemin (C-H). Confocal microscopy revealed three GFAP staining patterns, consisting of a filamentous network with little evidence of bundling (cell on left in A), or a network with some parts displaying large bundles and coils (cell on right in A and E). In overexpressing cells, GFAP formed large rods or comma-like structures (B,G). In cells with little GFAP bundling, synemin did not associate with the GFAP network, but formed dot-shaped accumulations (D). Synemin did associate with large GFAP bundles (F) or overexpression aggregates (H). In cells where only part of the GFAP network formed large bundles, synemin only associated with those parts (compare E with F). Bar, 10 μm.

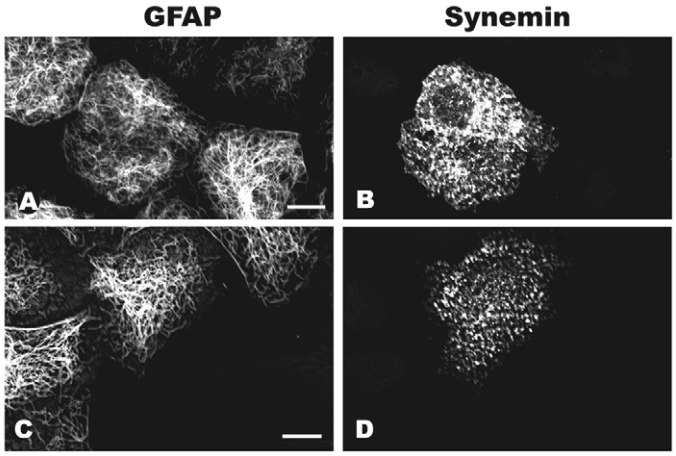

Fig. 9. SW13-cl2 cells stably transfected with GFAP and transiently transfected with α-synemin (A,B) or β-synemin (C,D). Double immunofluorescence staining for GFAP (A,C) and synemin (B,D) was performed 48 hours after transfection. Confocal microscopy revealed a filamentous GFAP network in most cells. Neither α- nor β-synemin associated with this network, instead forming dot-shaped structures not stained by anti-GFAP. Bar, 10 μm.

networks (Bellin et al., 1999; Titeux et al., 2001). These results suggest that, in astrocytes, vimentin functions as an adaptor that enables synemin to incorporate into GFAP-containing networks.

The induction of synemin synthesis in reactive astrocytes in wild-type mice after neurotrauma is consistent with our recent finding that human reactive astrocytes found around ischemic lesions or epileptic foci stain with synemin antibodies (Jing et al., 2005). We propose that synemin expression is part of the response of astrocytes to neurotrauma and other brain and spinal cord pathologies. Thus, along with nestin (Dahlstrand et al., 1992) and endothelin B receptors (Rogers et al., 1997), synemin might be a useful marker of reactive astrocytes.

Our immunofluorescence studies show that, in astrocyte cultures, synemin localizes over the entire IF network, irrespective of whether this network is assembled of vimentin or of vimentin and GFAP. In cultured astrocytes, synemin did not associate with α-actinin-rich cellular regions, as it does in muscle and astrocytoma cells (Sandoval et al., 1983; Bellin et al., 1999; Jing et al., 2005), or with focal contacts, as it does in hepatic stellate cells (Uyama et al., 2006). The factors determining synemin subcellular distribution in different cell types remain to be identified.

Synemin was not found in reactive astrocytes in *Gfap*$^{-/-}$*Vim*$^{-/-}$ mice after entorhinal cortex lesion or in brain tissue and cultured astrocytes from newborn *Gfap*$^{-/-}$*Vim*$^{-/-}$ and *Vim*$^{-/-}$ mice. This synemin expression profile is comparable to that of nestin, another type IV IF protein expressed by immature, reactive and malignant astrocytes (Dahlstrand et al., 1992; Lendahl et al., 1990; Frisen et al., 1995; Eliasson et al., 1999). In reactive astrocytes, nestin protein levels are high in wild-type mice, but are markedly reduced in *Gfap*$^{-/-}$*Vim*$^{-/-}$ and *Vim*$^{-/-}$ mice (Eliasson et al., 1999). Similarly, nestin protein levels are 80% lower in *Gfap*$^{-/-}$*Vim*$^{-/-}$ and *Vim*$^{-/-}$ cultured astrocytes than in wild-type and *Gfap*$^{-/-}$ cultured astrocytes (Eliasson et al., 1999).

Gene targeting studies in mice suggest that IF protein levels are decreased in the absence of a polymerization partner in cell types other than astrocytes. In the central nervous system, targeted gene ablation of neurofilament (NF)-M reduces NF-L protein levels by 30 to 90%, depending on the brain region (Jacomy et al., 1999; Elder et al., 1998). Genetic ablation of keratin 18 (K18) or K8 in mice also reduced protein levels for some of their keratin polymerization partners (Magin et al., 1998; Tao et al., 2003), and K2e protein was absent in transgenic mice expressing truncated, polymerization-incompetent K10 (Reichelt et al., 1997). In transfection experiments with cultured fibroblasts, the stability of a type II keratin required a polymerization partner (Kulesh et al., 1989).

Two lines of evidence strongly suggest that the stability of synemin in astrocytes also depends on the presence of a polymerization partner. First, because synemin incorporates into vimentin IF networks (Bellin et al., 1999; Titeux et al., 2001), it is significant that synemin was not detected in *Gfap*$^{-/-}$*Vim*$^{-/-}$ and *Vim*$^{-/-}$ astrocytes, but was present in *Gfap*$^{-/-}$ astrocytes at levels identical to those in wild-type astrocytes.

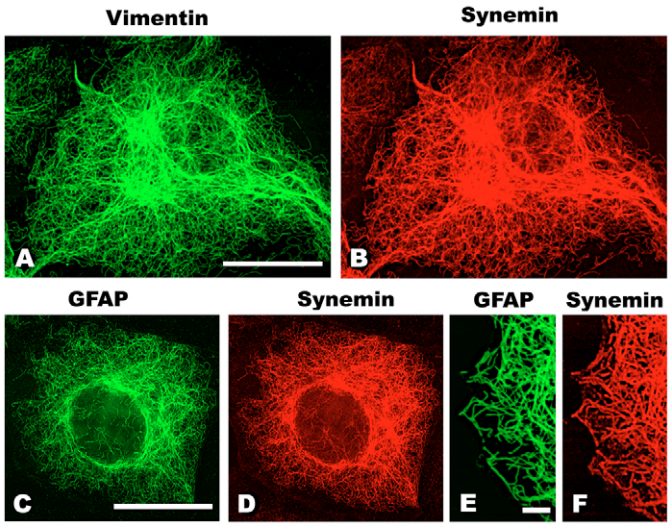

Fig. 10. SW13-cl2 cells stably transfected with GFAP and transiently cotransfected with vimentin and α-synemin. Double immunofluorescence staining for vimentin (A) and synemin (B) was performed 48 hours after transfection. Confocal microscopy revealed that synemin associated with the IF network in cells transfected with vimentin. (C,F) SW13-cl2 cells were stably transfected with vimentin and transiently cotransfected with GFAP and β-synemin, and double immunofluorescence staining with anti-GFAP (C,E) and anti-synemin (D,F) was performed 48 hours after transfection. In vimentin-containing cells transiently cotransfected with synemin and GFAP, confocal microscopy showed that synemin incorporated into the entire GFAP network (D,F). (E,F) Synemin also incorporated into the most peripheral area of the GFAP network, where it is the least dense. Bars, 10 μm (A-D); 1 μm (E,F).

Moreover, our immunofluorescence and biochemical studies revealed that synemin incorporation into the vimentin IF network in *Gfap*$^{-/-}$ astrocytes was indistinguishable from that in wild-type astrocytes. Second, synemin did not accumulate in *Vim*$^{-/-}$ cells, even though they possess a filamentous GFAP network (Eliasson et al., 1999). That synemin does not incorporate into a GFAP network was demonstrated directly by the finding that in SW13-cl2 cells cotransfected with synemin and GFAP cDNAs, synemin accumulated as punctate inclusions that were independent of the GFAP network.

Synemin mRNA levels were not reduced in astrocytes deficient in GFAP and/or vimentin. This finding establishes that synemin protein levels in vimentin-deficient astrocytes are regulated post-transcriptionally. This may be a general mechanism by which IF protein levels are regulated in the absence of polymerization partners, as post-transcriptional regulation is also responsible for decreased nestin, NF-L and keratin protein levels after the genetic ablation of vimentin, NF-M and of specific keratin pair members, respectively (Reichelt et al., 1997; Elder et al., 1998; Magin et al., 1998; Eliasson et al., 1999; Jacomy et al., 1999; Tao et al., 2003).

Although synemin did not accumulate in astrocytes lacking vimentin, it did form cytoplasmic inclusions in SW13-cl2 adrenocarcinoma cells lacking vimentin. In this cell line, the lack of IF protein is not caused by targeted IF gene disruption, but by the inactivation of two members of the trithorax pathway, resulting in the inactivation of many genes involved in maintaining a differentiated state (Yamamichi-Nishina et al., 2003). Conceivably, the products of some of these genes may also be involved in post-transcriptional control of IF protein accumulation. In their absence, synemin may accumulate in SW13-cl2 cells without a polymerization partner. In any case, our experiments with GFAP-transfected SW13-cl2 cells showed that synemin mRNA can be translated in the absence of vimentin. Thus, in *Gfap*$^{-/-}$*Vim*$^{-/-}$ and *Vim*$^{-/-}$ astrocytes, synemin may fail to accumulate because of post-translational regulatory mechanisms. Such mechanisms are responsible for the failure of K8 protein to accumulate in fibroblasts transfected with a K8 cDNA (Kulesh et al., 1989).

Our biochemical experiments and those of others (Bellin et al., 1999) suggest that synemin associates with vimentin IF networks by copolymerizing with vimentin rather than by binding to vimentin IFs after vimentin polymerization. Although synemin can integrate into vimentin IF networks (Bellin et al., 1999; Titeux et al., 2001), our transfection experiments demonstrate that synemin does not associate with a normal fibrillar GFAP network in vivo. This is surprising because synemin had some capacity to interact with GFAP in our in vitro biochemical experiments. However, those experiments also suggested that synemin may not copolymerize with GFAP. Instead, it may only associate with GFAP IFs after GFAP polymerization, as similar amounts of synemin were recovered in the GFAP IF pellet in ultracentrifugation assays, regardless of whether synemin was mixed with GFAP before GFAP polymerization or added to GFAP IFs after GFAP polymerization. Thus, in the copolymerization experiments, the synemin in the pellets may reflect its association with GFAP IFs after GFAP polymerization rather than its incorporation into GFAP IFs during GFAP polymerization. Our transfection experiments showed that this binding of synemin to GFAP IFs did not take place along a GFAP filamentous network, but occurred in structures arising from GFAP overexpression, such as GFAP aggregates and cables. Synemin does not play a role in the formation of these structures because they are present in cells transfected with GFAP only, as we showed here, and in the case of GFAP cables, in *Vim*$^{-/-}$ astrocytes (Eliasson et al., 1999), which we showed are devoid of synemin.

Other differences between the in vitro and in vivo behavior of IF proteins have been reported. NF-L, for instance, forms homopolymers in vitro, but not in vivo (Ching and Liem, 1993; Lee et al., 1993). Such differences may occur because IF assembly in cells commences during the translation of IF proteins (Moon and Lazarides, 1983; Isaacs et al., 1989; Chang et al., 2006). Pulse-chase studies in avian erythroid cells showed that the elongation of vimentin IF generates sites for the incorporation of synemin (Moon and Lazarides, 1983). Such translational interactions may be especially important for understanding how synemin incorporates into IF networks in cells.

Transient cotransfection of synemin and vimentin into SW13-cl2 cells stably transfected with GFAP showed that synemin can incorporate into a pre-existing GFAP network in the presence of vimentin. Similarly, transient cotransfection of synemin and GFAP into SW13-cl2 cells stably transfected with vimentin showed that a pre-existing vimentin IF network can serve as a scaffold for the incorporation of GFAP and synemin. These results suggest that one function of vimentin in

astrocytes is to permit the incorporation of synemin into GFAP-containing IFs. The pattern of synemin expression in astrocytes also supports this possibility. Synemin is expressed in astrocytes when vimentin is also present, such as during development, in astrocytomas and, as we have shown here, in reactive astrocytes in neurotrauma. In adults, synemin was not detected in mature cerebral astrocytes (Sultana et al., 2000; Jing et al., 2005) (this study), but is present in the optic nerve astrocytes (Hirako et al., 2003), which coexpress GFAP and vimentin (Dahl et al., 1981; Calvo et al., 1990).

Our findings establish that GFAP and vimentin interact differently with synemin in vivo. First, in astrocytes, expression of vimentin, but not of GFAP, was crucial for synemin accumulation, as shown by differences in synemin protein levels in the brains of wild-type, *Vim*$^{-/-}$, *Gfap*$^{-/-}$*Vim*$^{-/-}$ and *Gfap*$^{-/-}$ mice. Second, synemin was not incorporated into a GFAP filamentous network as it was into a vimentin network. This finding may reflect differences in the dynamic properties of GFAP and vimentin filamentous networks and/or the fact that the head domains of vimentin and GFAP, which are important for polymerization, diverge at the primary sequence level (Traub and Vorgias, 1984; Ralton et al., 1994; Herrmann et al., 1996).

However, the tail and rod domains of GFAP and vimentin share ~80% homology. They are also highly homologous with the tail and rod domains of desmin, the muscle-specific type III IF protein that coexists with synemin in muscle cells during development and in adulthood (Price and Lazarides, 1993; Bilak et al., 1998). In its in vitro interaction with synemin, desmin resembles vimentin more than GFAP because, in biochemical assays, synemin copolymerizes with desmin but binds only minimally to preformed desmin IFs (Bellin et al., 1999). In addition, desmin may, like vimentin, stabilize synemin because, in smooth muscle cells co-expressing desmin and vimentin, synemin is found in *Vim*$^{-/-}$ or *Des*$^{-/-}$, but not in *Vim*$^{-/-}$*Des*$^{-/-}$ cells (Xue et al., 2004). Skeletal and cardiac muscle cells also co-express synemin and desmin, but not vimentin, further suggesting that vimentin is not required for synemin to incorporate into a desmin IF network. In these cells, the absence of desmin leads to greatly reduced synemin protein levels (Carlsson et al., 2000; Xue et al., 2004).

In conclusion, this study demonstrates that neurotrauma induces synemin expression in reactive astrocytes. Importantly, our results in transgenic mice lacking vimentin and/or GFAP also shed light on the functional significance of vimentin upregulation in reactive astrocytes. Specifically, our findings suggests that vimentin is required for synemin to accumulate in astrocytes in response to injury. However, the closely related IF protein GFAP does not perform this function, because vimentin and GFAP differ in their capacity to interact with synemin and to incorporate it into a normal filamentous IF network. The functional significance of synemin expression in reactive astrocytes remains to be determined. However, our findings in cultured astrocytes, whose IF protein composition resembles that of reactive astrocytes, suggest that synemin does not link the IF network to structures rich in α-actinin or vinculin in astrocytes, as it does in other cell types (Sandoval et al., 1983; Bellin et al., 1999; Jing et al., 2005; Uyama et al., 2006). Synemin, however, also binds α-dystrobrevin (Mizuno et al., 2001) protein kinase A regulatory subunit II (Russell et al., 2006), as well as dystrophin and urotrophin (Bhosle et al., 2006). Future investigations will examine whether synemin interacts with some of these proteins in reactive astrocytes.

Materials and Methods

Mice

Mice carrying a null mutation in the GFAP and/or vimentin gene and wild-type controls have been described (Colucci-Guyon et al., 1994; Pekny et al., 1995; Pekny et al., 1999). All mice were on a mixed genetic background (C57Bl/6-129Sv-129Ola).

Surgery

Unilateral entorhinal cortex lesioning was performed in 15-month-old female mice. This lesion partly interrupts the perforant pathway, which innervates the molecular layer in the ipsilateral dentate gyrus of the hippocampus. Axonal degeneration triggers astrocyte activation in the dentate gyrus, an area not directly affected by the trauma. The surgical procedure was performed as described (Stone et al., 1998; Wilhelmsson et al., 2004), with the coordinates +3.6 mm lateral and –0.2 mm posterior to lambda for insertion of the wireknife. The brains were fixed and dissected 4 or 14 days after lesioning, as described (Wilhelmsson et al., 2004).

Cell culture

Primary astrocytes were obtained from the brain hemispheres of 2-day-old mice as described (Pekny et al., 1998). SW13-cl2 adrenocortical carcinoma cells (Sarria et al., 1990) were a kind gift from Robert Evans (Department of Pathology, University of Colorado Health Sciences Center, Denver, CO). Cells were grown in Dulbecco's modified Eagle's medium (DMEM) supplemented as described (Sultana et al., 2000).

Antibodies and immunofluorescence

Rabbit antibodies against the C-terminus of human α-synemin were raised and affinity-purified as reported (Jing et al., 2005). Other primary antibodies included: mouse monoclonal anti-human vimentin clone V9 (Sigma), mouse monoclonal anti-vinculin (ICN), chicken anti-human and rodent vimentin (Chemicon), mouse monoclonal anti-GFAP clone GA5 (Sigma), mouse monoclonal anti-α-smooth muscle actin (Sigma), and rabbit anti-actin (Sigma). The secondary antibodies were affinity-purified goat anti-mouse or anti-rabbit IgG or anti-chicken IgY conjugated to peroxidase (Kirkegaard & Perry), or Alexa Fluor-488 or Alexa Fluor-588 (Invitrogen). Nuclei were stained with TOPRO-3 (Invitrogen).

Brain sections and cells plated on glass coverslips were fixed and stained for immunofluorescence as detailed earlier (Jing et al., 2005; Wilhelmsson et al., 2004). Confocal microscope observations were performed as described (Jing et al., 2005; Wilhelmsson et al., 2004).

Preparation of total, cytoskeletal and cytosolic protein samples

Total protein samples for SDS-PAGE were prepared as described by Sultana et al. (Sultana et al., 1998). For cytoskeletal and cytosolic protein samples, cells were lysed in lysis buffer (150 μl per 10 cm^2) [10 mM Tris-Cl (pH 7.4), 140 mM NaCl, 1% (v/v) Triton X-100, 2 mM EGTA] and protease inhibitors as described (Jing et al., 2005). Centrifugation at 14,000 ***g*** for 15 minutes yielded a pellet enriched in cytoskeletal proteins and a supernatant containing cytosolic proteins. Gel loading buffer (150 μl) was added to each supernatant, and pelleted proteins were dissolved in 300 μl of a 1:1 mixture of lysis buffer and gel loading buffer.

Protein concentration determination, SDS-PAGE, western blotting and densitometry

Protein concentrations were measured as described (Jing et al., 2005). For comparison of protein expression levels, 5 μg of total cellular proteins were loaded per lane. To determine whether IF proteins partition between cytoskeletal and cytosolic compartments, equal volumes of protein samples were loaded. Proteins were separated on 4-15% gradient SDS-polyacrylamide gels. Gels were stained with GelCode Blue (Pierce) or processed for western blotting (Jing et al., 2005). Densitometric and statistical analysis were performed as described (Sultana et al., 1998).

Qualitative and quantitative PCR

Total RNA was purified from tissues with the MELT Total RNA Isolation System (Ambion) and from cultured cells with the High Pure RNA Isolation Kit (Roche). Genomic DNA contamination was avoided by treating samples with RNase-free DNase I. cDNA synthesis was performed with Thermoscript reverse transcriptase (Invitrogen) using an oligo(dT)$_{20}$ primer. RT-PCR of murine synemin isoforms was performed using the conditions and the P2 and P5 primers described by Xue et al. (Xue et al., 2004). These primers amplify all synemin isoforms.

Quantitative PCR for synemin was performed with a TaqMan assay utilizing the fluorigenic probe 5′-AGCCTTCTTCCCTGACCCGTGTGT-3′ conjugated to TAMRA and 6FAM, and the primers 5′-GAGGATGCCATCTTCAGGTAGG-3′ and 5′-AGCCGTTCTGTGTTTCTCTTATAC-3′. These primers and the probe allow quantitation of all synemin isoforms in one reaction. Glyceraldehyde-3-phosphate

dehydrogenase (GAPDH) served as endogenous control, using the primers and probe provided by ABI. Quantitative PCR was performed with an ABI Prism 7700 and data were analyzed with the ABI 7700 Sequence Detection System using the comparative Ct method. Values are expressed as means ± s.e.m. of three to four separate experiments; differences were analyzed by *t*-test or one-way analysis of variance (ANOVA).

Cloning human GFAP, vimentin and α- and β-synemin cDNAs into expression vectors

mRNA purification from U-373 MG human glioblastoma cells and cDNA synthesis were performed following standard procedures, using the following gene-specific reverse primers: 5′-AGCCCAGGAGTTCAAGGTCA-3′ (GFAP), 5′-AAACTGC-AGAAAGGCACTTGA-3′ (vimentin) and 5′-AAATTGACCATGCCGGGAGTA-3′ (synemin). PCR reactions were conducted with Advantage-GC cDNA polymerase mix (BD Biosciences) and, for each cDNA, with the reverse primer used for cDNA synthesis and the corresponding gene-specific forward primers: 5′-ACGATGGAGAGGAGACGCAT-3′ (GFAP), 5′-ATGTCCACCAGGTCCGTGTC-3′ (vimentin) and 5′-GAGGACGAGACCGGGACAAGA-3′ (synemin). For synemin, this yielded products of 4.9 kb (α-synemin) and 3.9 kb (β-synemin). PCR products were inserted by topocloning into the eukaryotic expression vector pcDNA3.1/V5-His TOPO (Invitrogen). The PCR products included a stop codon at the end of the reading frame for protein expression without the V5-His tag.

Vimentin and GFAP PCR products were also inserted by topocloning into the prokaryotic expression vector pTrcHis2-TOPO (Invitrogen). For α- and β-synemin, we inserted into this vector cDNA obtained by PCR using the primers 5′-ATGCTGTCCTTGCGGCTG-3′ and 5′-AAATTGACCATGCCGGGAGTA-3′. The PCR products included the stop codon at the end of the reading frame, for protein expression without the tag. Because of the sequence of the cloning site and, for GFAP, of the forward primer, the translated proteins contained at their N-terminus the additional amino acids MAL, for vimentin and α- and β-synemin, and MALT, for GFAP. For bacterial expression, pTrcHis2-TOPO constructs were transduced into BL21-CodonPlus-RIL *Escherichia coli* (Stratagene).

DNA sequencing and BLAST search revealed that our human GFAP and vimentin cDNAs encode amino-acid sequences identical to J04569 and X56134, respectively. For α- and β-synemin, our cDNAs encode proteins identical to O15061 and NP 056101, respectively.

Purification of bacterially expressed human GFAP, vimentin and α- and β-synemin

All buffers included the protease inhibitors described in Jing et al. (Jing et al., 2005). GFAP, vimentin and α- and β-synemin synthesis was induced for 3 hours with 1 mM IPTG. The bacteria were pelleted at 5000 ***g*** for 10 minutes, resuspended in 10 mM MES, pH 6.0, 5 mM EDTA and 0.5 mM DTT, lysed with a French press, sonicated and centrifuged at 15,000 ***g*** for 15 minutes. The pellets were resuspended in 10 mM HEPES, pH 7.0, 1.5 M KCl, 5 mM EDTA, 1% Triton X-100 and 0.5 mM DTT and centrifuged at 15,000 ***g*** for 15 minutes. This procedure was repeated twice, and the final pellet was resuspended in the same buffer, but without Triton X-100, and centrifuged at 15,000 ***g*** for 15 minutes. The pellet was extracted with buffer G (6M guanidine HCl, 20 mM Tris-HCl, pH 7.8, 500 mM NaCl, 5 mM EDTA and 0.5 mM DTT).

For GFAP and vimentin, buffer G extracts were dialyzed against 2 mM Tris-HCl, pH 8.0, 1 mM EDTA and 0.5 mM DTT, and ultracentrifuged at 100,000 ***g*** for 30 minutes. GFAP or vimentin IF assembly was induced by adding 140 mM NaCl to the supernatants. After 1 hour of incubation, GFAP or vimentin IFs were collected by ultracentrifugation at 100,000 ***g*** for 30 minutes. The IF pellet was solubilized in buffer U (8 M urea, 50 mM Tris-HCl, pH 8.0, 1 mM DTT and 5 mM EDTA), and two to three additional polymerization cycles were performed.

For α- and β-synemins, buffer G extracts were dialyzed against buffer P (10 mM Tris-HCl, pH 7.8, 5 mM EDTA, 140 mM NaCl), and centrifuged at 15,000 ***g*** for 30 minutes. Urea was added to the supernatant to reach 6 M final concentration, and purified vimentin in buffer U was added to this solution using the empirical formula, A [vimentin (mg)]=VD/60, where V (ml) is the volume of the supernatant and D is its optical density at 280 nm. The rationale for this step is to use synemin capacity to copolymerize with vimentin (Bellin et al., 1999; Titeux et al., 2001) to separate it from bacterial proteins. Copolymerization was induced by dialysis against buffer P, and IFs were pelleted by ultracentrifugation at 100,000 ***g*** for 30 minutes.

The final IF protein pellets dissolved in buffer U were loaded onto either a 2.5×100 cm Sephacryl S-200 (GFAP and vimentin) or a 1.5×100 cm Sephacryl S-300 (α- and β-synemin) gel filtration column equilibrated with buffer U. Chromatography was run at a flow rate of 7.5 ml/hour (GFAP and vimentin) or 9 ml/hour (α- and β-synemin). Fractions containing a single band of appropriate size and immunoreactivity were identified by SDS-PAGE and western blotting.

Binding and cosedimentation assays

For blot overlays, 0.2 μg each of GFAP, vimentin and platelet actin (Cytoskeleton) were loaded onto a 4-15% SDS-polyacrylamide gel and transferred to nitrocellulose filters. For dot-blot assays, proteins were dialyzed against 2 mM Tris-HCl (pH 7.2) and 0.5 mM DTT, and 5, 1, 0.5 or 0.1 μg of each protein was spotted onto nitrocellulose filters. The filters were then overlayed with synemin and incubated with antibodies as described (Hirako et al., 2003).

For copolymerization assays, mixtures of synemin and either GFAP or vimentin were assembled in buffer U (see above) at a 1:100 molar ratio (synemin:GFAP or vimentin), with GFAP or vimentin at a final concentration of 0.5 mg/ml. Control samples contained only synemin at the same final concentration as in the protein mixtures. Vimentin or GFAP IF assembly was obtained by dialysis against buffer P (2 mM Tris-HCl, pH 7.2, 140 mM NaCl and 0.5 mM DTT), and the samples were ultracentrifuged at 100,000 ***g*** for 30 minutes.

To determine whether synemin binds to GFAP or vimentin IFs after they have polymerized, synemin (0.1 mg/ml), GFAP (0.5 mg/ml) and vimentin (0.5 mg/ml) in buffer U (see above) were individually dialyzed against buffer P. This induces the assembly of GFAP or vimentin IFs, but not of synemin (Bilak et al., 1998). The synemin sample was ultracentrifuged at 100,000 ***g*** for 30 minutes. The supernatant (25 μl) was added to 75 μl of either GFAP or vimentin IF, or buffer P for control. Under these conditions, the molar ratio of synemin:GFAP or vimentin was in the 1:50-1:100 range. After a 1-hour incubation at 25°C, samples were ultracentrifuged at 100,000 ***g*** for 30 minutes.

SDS gel-loading buffer was added to supernatant and pellet proteins to the same final volume, and equal volumes were loaded on gels for comparison.

Transfection of SW13-cl2 cells

Plasmid DNA was obtained with the endotoxin-free plasmid purification kit from Qiagen (Valencia, CA). For stable transfection, the plasmids were linearized with *Mlu*I (for α- and β-synemin) or *Mfe*I (for GFAP and vimentin). Transfections were performed on SW13-cl2 cells by adding for 4 hours in 10 cm^2 well 2 μg of DNA forming a 1:3 (w/v) complex with Fugene 6 reagent (Roche). After 1-2 days, cells were stained by immunofluorescence or, for stable transfection, trypsinized and plated into medium containing 1.5 mg/ml geneticin. After ~2 weeks, geneticin-resistant clones were lifted off the dishes by trypsinization using cloning cylinders.

We thank Paula Polk and Lijia Yin from the LSU-Shreveport core facility for assistance with quantitative RT-PCR experiments. This work was supported by National Institutes of Health grant NS-35317 to O.S., the Swedish Medical Society (16850) to U.W. and the Swedish Research Council (11548), Hjärnfoden, LUA/ALF Göteborg, Stroke Foundation and Torsten and Ragnar Söderbergs Foundations to M.P.

References

Bellin, R. M., Sernett, S. W., Becker, B., Ip, W., Huiatt, T. W. and Robson, R. M. (1999). Molecular characteristics and interactions of the intermediate filament protein synemin. Interactions with alpha-actinin may anchor synemin-containing heterofilaments. *J. Biol. Chem.* **274**, 29493-29499.

Bellin, R. M., Huiatt, T. W., Critchley, D. R. and Robson, R. M. (2001). Synemin may function to directly link muscle cell intermediate filaments to both myofibrillar Z-lines and costameres. *J. Biol. Chem.* **276**, 32330-32337.

Bhosle, R. C., Michele, D. E., Campbell, K. P., Li, Z. and Robson, R. M. (2006). Interactions of intermediate filament protein synemin with dystrophin and utrophin. *Biochem. Biophys. Res. Commun.* **346**, 768-777.

Bilak, S. R., Sernett, S. W., Bilak, M. M., Bellin, R. M., Stromer, M. H., Huiatt, T. W. and Robson, R. M. (1998). Properties of the novel intermediate filament protein synemin and its identification in mammalian muscle. *Arch. Biochem. Biophys.* **355**, 63-76.

Calvo, J. L., Carbonell, A. L. and Boya, J. (1990). Coexpression of vimentin and glial fibrillary acidic protein in astrocytes of the adult rat optic nerve. *Brain Res.* **532**, 355-357.

Carlsson, L., Li, Z. L., Paulin, D., Price, M. G., Breckler, J., Robson, R. M., Wiche, G. and Thornell, L. E. (2000). Differences in the distribution of synemin, paranemin, and plectin in skeletal muscles of wild-type and desmin knock-out mice. *Histochem. Cell Biol.* **114**, 39-47.

Chang, L. and Goldman, R. D. (2004). Intermediate filaments mediate cytoskeletal crosstalk. *Nat. Rev. Mol. Cell Biol.* **5**, 601-613.

Chang, L., Shav-Tal, Y., Trcek, T., Singer, R. H. and Goldman, R. D. (2006). Assembling an intermediate filament network by dynamic cotranslation. *J. Cell Biol.* **172**, 747-758.

Chen, W. J. and Liem, R. K. H. (1994). The endless story of the glial fibrillary acidic protein. *J. Cell Sci.* **107**, 2299-2311.

Ching, G. Y. and Liem, R. K. H. (1993). Assembly of type IV neuronal intermediate filaments in nonneuronal cells in the absence of preexisting cytoplasmic intermediate filaments. *J. Cell Biol.* **122**, 1323-1335.

Colucci-Guyon, E., Portier, M. M., Dunia, I., Paulin, D., Pournin, S. and Babinet, C. (1994). Mice lacking vimentin develop and reproduce without an obvious phenotype. *Cell* **79**, 679-694.

Coulombe, P. A. and Wong, P. (2004). Cytoplasmic intermediate filaments revealed as dynamic and multipurpose scaffolds. *Nat. Cell Biol.* **6**, 699-706.

Dahl, D., Bignami, A., Weber, K. and Osborn, M. (1981). Filament proteins in rat optic

nerves undergoing Wallerian degeneration: localization of vimentin, the fibroblastic 100-A filament protein, in normal and reactive astrocytes. *Exp. Neurol*. **73**, 496-506.
Dahlstrand, J., Collins, V. P. and Lendahl, U. (1992). Expression of the class VI intermediate filament nestin in human central nervous system tumors. *Cancer Res*. **52**, 5334-5341.
Elder, G. A., Friedrich, V. L., Jr, Bosco, C., Kang, P., Gourov, A., Tu, P. H., Lee, V. M. and Lazzarini, R. A. (1998). Absence of the mid-sized neurofilament subunit decreases axonal calibers, levels of light neurofilament (NF-L), and neurofilament content. *J. Cell Biol.* **141**, 727-739.
Eliasson, C., Sahlgren, C., Berthold, C. H., Stakeberg, J., Celis, J. E., Betsholtz, C., Eriksson, J. E. and Pekny, M. (1999). Intermediate filament protein partnership in astrocytes. *J. Biol. Chem.* **274**, 23996-24006.
Eng, L. F., Ghirnikar, R. S. and Lee, Y. L. (2000). Glial fibrillary acidic protein: GFAP-thirty-one years (1969-2000). *Neurochem. Res*. **25**, 1439-1451.
Frisen, J., Johansson, C. B., Torok, C., Risling, M. and Lendahl, U. (1995). Rapid, widespread, and long-lasting induction of nestin contributes to the generation of glial scar tissue after CNS injury. *J. Cell Biol*. **131**, 453-464.
Herrmann, H. and Aebi, U. (2004). Intermediate filaments: molecular structure, assembly mechanism, and integration into functionally distinct intracellular scaffolds. *Annu. Rev. Biochem.* **73**, 749-789.
Herrmann, H., Haner, M., Brettel, M., Muller, S. A., Goldie, K. N., Fedtke, B., Lustig, A., Franke, W. W. and Aebi, U. (1996). Structure and assembly properties of the intermediate filament protein vimentin: the role of its head, rod and tail domains. *J. Mol. Biol.* **264**, 933-953.
Hirako, Y., Yamakawa, H., Tsujimura, Y., Nishizawa, Y., Okumura, M., Usukura, J., Matsumoto, H., Jackson, K. W., Owaribe, K. and Ohara, O. (2003). Characterization of mammalian synemin, an intermediate filament protein present in all four classes of muscle cells and some neuroglial cells: co-localization and interaction with type III intermediate filament proteins and keratins. *Cell Tissue Res.* **313**, 195-207.
Isaacs, W. B., Cook, R. K., Van Atta, J. C., Redmond, C. M. and Fulton, A. B. (1989). Assembly of vimentin in cultured cells varies with cell type. *J. Biol. Chem*. **264**, 17953-17960.
Izmiryan, A., Cheraud, Y., Khanamiryan, L., Leterrier, J. F., Federici, T., Peltekian, E., Moura-Neto, V., Paulin, D., Li, Z. and Xue, Z. G. (2006). Different expression of synemin isoforms in glia and neurons during nervous system development. *Glia* **54**, 204-213.
Jacomy, H., Zhu, Q., Couillard-Despres, S., Beaulieu, J. M. and Julien, J. P. (1999). Disruption of type IV intermediate filament network in mice lacking the neurofilament medium and heavy subunits. *J. Neurochem*. **73**, 972-984.
Jing, R., Pizzolato, G., Robson, R. M., Gabbiani, G. and Skalli, O. (2005). Intermediate filament protein synemin is present in human reactive and malignant astrocytes and associates with ruffled membranes in astrocytoma cells. *Glia* **50**, 107-120.
Kooijman, M., van Amerongen, H., Traub, P., van Grondelle, R. and Bloemendal, M. (1995). The assembly state of the intermediate filament proteins desmin and glial fibrillary acidic protein at low ionic strength. *FEBS Lett.* **358**, 185-188.
Kulesh, D. A., Cecena, G., Darmon, Y. M., Vasseur, M. and Oshima, R. G. (1989). Posttranslational regulation of keratins: degradation of mouse and human keratins 18 and 8. *Mol. Cell. Biol*. **9**, 1553-1565.
Lane, E. B. and Pekny, M. (2004). Stress models for the study of intermediate filament function. *Methods Cell Biol.* **78**, 229-264.
Lee, M. K., Xu, Z., Wong, P. C. and Cleveland, D. W. (1993). Neurofilaments are obligate heteropolymers in vivo. *J. Cell Biol*. **122**, 1337-1350.
Lendahl, U., Zimmerman, L. B. and McKay, R. D. (1990). CNS stem cells express a new class of intermediate filament protein. *Cell* **60**, 585-595.
Magin, T. M., Schroder, R., Leitgeb, S., Wanninger, F., Zatloukal, K., Grund, C. and Melton, D. W. (1998). Lessons from keratin 18 knockout mice: formation of novel keratin filaments, secondary loss of keratin 7 and accumulation of liver-specific keratin 8-positive aggregates. *J. Cell Biol*. **140**, 1441-1451.
Marvin, M. J., Dahlstrand, J., Lendahl, U. and McKay, R. D. (1998). A rod end deletion in the intermediate filament protein nestin alters its subcellular localization in neuroepithelial cells of transgenic mice. *J. Cell Sci*. **111**, 1951-1961.
Mizuno, Y., Thompson, T. G., Guyon, J. R., Lidov, H. G., Brosius, M., Imamura, M., Ozawa, E., Watkins, S. C. and Kunkel, L. M. (2001). Desmuslin, an intermediate filament protein that interacts with alpha-dystrobrevin and desmin. *Proc. Natl. Acad. Sci. USA* **98**, 6156-6161.
Moon, R. T. and Lazarides, E. (1983). Synthesis and post-translational assembly of intermediate filaments in avian erythroid cells: vimentin assembly limits the rate of synemin assembly. *Proc. Natl. Acad. Sci. USA* **80**, 5495-5499.
Omary, M. B., Coulombe, P. A. and McLean, W. H. (2004). Intermediate filament proteins and their associated diseases. *N. Engl. J. Med*. **351**, 2087-2100.
Pekny, M. and Pekna, M. (2004). Astrocyte intermediate filaments in CNS pathologies and regeneration. *J. Pathol*. **204**, 428-437.
Pekny, M. and Wilhelmsson, U. (2006). Intermediate filaments in astrocytes in health and disease. In *Intermediate Filaments* (ed. J. Paramio), pp. 10-26. Texas: Landes Bioscience/Eurekah.com.
Pekny, M., Leveen, P., Pekna, M., Eliasson, C., Berthold, C. H., Westermark, B. and Betsholtz, C. (1995). Mice lacking glial fibrillary acidic protein display astrocytes devoid of intermediate filaments but develop and reproduce normally. *EMBO J.* **14**, 1590-1598.
Pekny, M., Eliasson, C., Chien, C. L., Kindblom, L. G., Liem, R., Hamberger, A. and Betsholtz, C. (1998). GFAP-deficient astrocytes are capable of stellation in vitro when cocultured with neurons and exhibit a reduced amount of intermediate filaments and an increased cell saturation density. *Exp. Cell Res*. **239**, 332-343.
Pekny, M., Johansson, C. B., Eliasson, C., Stakeberg, J., Wallen, A., Perlmann, T., Lendahl, U., Betsholtz, C., Berthold, C. H. and Frisen, J. (1999). Abnormal reaction to central nervous system injury in mice lacking glial fibrillary acidic protein and vimentin. *J. Cell Biol*. **145**, 503-514.
Price, M. G. and Lazarides, E. (1983). Expression of intermediate filament-associated proteins paranemin and synemin in chicken development. *J. Cell Biol*. **97**, 1860-1874.
Quinlan, R. A. and Franke, W. W. (1983). Molecular interactions in intermediate-sized filaments revealed by chemical cross-linking. Heteropolymers of vimentin and glial filament protein in cultured human glioma cells. *Eur. J. Biochem*. **132**, 477-484.
Ralton, J. E., Lu, X., Hutcheson, A. M. and Quinlan, R. A. (1994). Identification of two N-terminal non-alpha-helical domain motifs important in the assembly of glial fibrillary acidic protein. *J. Cell Sci*. **107**, 1935-1948.
Reichelt, J., Bauer, C., Porter, R., Lane, E. and Magin, V. (1997). Out of balance: consequences of a partial keratin 10 knockout. *J. Cell Sci*. **110**, 2175-2186.
Rogers, S. D., Demaster, E., Catton, M., Ghilardi, J. R., Levin, L. A., Maggio, J. E. and Mantyh, P. W. (1997). Expression of endothelin-B receptors by glia in vivo is increased after CNS injury in rats, rabbits, and humans. *Exp. Neurol*. **145**, 180-195.
Russell, M. A., Lund, L. M., Haber, R., McKeegan, K., Cianciola, N. and Bond, M. (2006). The intermediate filament protein, synemin, is an AKAP in the heart. *Arch. Biochem. Biophys.* **456**, 204-215.
Rutka, J. T., Murakami, M., Dirks, P. B., Hubbard, S. L., Becker, L. E., Fukuyama, K., Jung, S., Tsugu, A. and Matsuzawa, K. (1997). Role of glial filaments in cells and tumors of glial origin: a review. *J. Neurosurg*. **87**, 420-430.
Sandoval, I. V., Colaco, C. A. L. S. and Lazarides, E. (1983). Purification of intermediate filament-associated protein, synemin, from chicken smooth muscle. Studies of its physicochemical properties, interaction with desmin and phosphorylation. *J. Biol. Chem.* **256**, 2568-2576.
Sarria, A. J., Nordeen, S. K. and Evans, R. M. (1990). Regulated expression of vimentin cDNA in cells in the presence and absence of a preexisting vimentin filament network. *J. Cell Biol*. **111**, 553-565.
Schweitzer, S. C., Klymkowsky, M. W., Bellin, R. M., Robson, R. M., Capetanaki, Y. and Evans, R. M. (2001). Paranemin and the organization of desmin filament networks. *J. Cell Sci.* **114**, 1079-1089.
Steinert, P. M., Chou, Y. H., Prahlad, V., Parry, D. A., Marekov, L. N., Wu, K. C., Jang, S. I. and Goldman, R. D. (1999). A high molecular weight intermediate filament-associated protein in BHK-21 cells is nestin, a type VI intermediate filament protein. Limited co-assembly in vitro to form heteropolymers with type III vimentin and type IV alpha-internexin. *J. Biol. Chem.* **274**, 9881-9890.
Stone, D. J., Rozovsky, I., Morgan, T. E., Anderson, C. P. and Finch, C. E. (1998). Increased synaptic sprouting in response to estrogen via an apolipoprotein E-dependent mechanism: implications for Alzheimer's disease. *J. Neurosci*. **18**, 3180-3185.
Sultana, S., Zhou, R., Sadagopan, M. S. and Skalli, O. (1998). Effects of growth factors and basement membrane proteins on the phenotype of U-373 MG glioblastoma cells as determined by the expression of intermediate filament proteins. *Am. J. Pathol.* **153**, 1157-1168.
Sultana, S., Sernett, S. W., Bellin, R. M., Robson, R. M. and Skalli, O. (2000). The intermediate filament protein synemin is transiently expressed in a subpopulation of astrocytes during development. *Glia* **30**, 143-153.
Tao, G. Z., Toivola, D. M., Zhong, B., Michie, S. A., Resurreccion, E. Z., Tamai, Y., Taketo, M. M. and Omary, M. B. (2003). Keratin-8 null mice have different gallbladder and liver susceptibility to lithogenic diet-induced injury. *J. Cell Sci.* **116**, 4629-4638.
Titeux, M., Brocheriou, V., Xue, Z., Gao, J., Pellissier, J. F., Guicheney, P., Paulin, D. and Li, Z. (2001). Human synemin gene generates splice variants encoding two distinct intermediate filament proteins. *Eur. J. Biochem*. **268**, 6435-6449.
Traub, P. and Vorgias, C. E. (1983). Involvement of the N-terminal polypeptide of vimentin in the formation of intermediate filaments. *J. Cell Sci.* **63**, 43-67.
Uyama, N., Zhao, L., Van Rossen, E., Hirako, Y., Reynaert, H., Adams, D. H., Xue, Z., Li, Z., Robson, R., Pekny, M. et al. (2006). Hepatic stellate cells express synemin, a protein bridging intermediate filaments to focal adhesions. *Gut* **55**, 1276-1289.
Wang, E., Cairncross, J. G. and Liem, R. K. (1984). Identification of glial filament protein and vimentin in the same intermediate filament system in human glioma cells. *Proc. Natl. Acad. Sci. USA* **81**, 2102-2106.
Wilhelmsson, U., Li, L., Pekna, M., Berthold, C. H., Blom, S., Eliasson, C., Renner, O., Bushong, E., Ellisman, M., Morgan, T. E. et al. (2004). Absence of glial fibrillary acidic protein and vimentin prevents hypertrophy of astrocytic processes and improves post-traumatic regeneration. *J. Neurosci*. **24**, 5016-5021.
Xue, Z. G., Cheraud, Y., Brocheriou, V., Izmiryan, A., Titeux, M., Paulin, D. and Li, Z. (2004). The mouse synemin gene encodes three intermediate filament proteins generated by alternative exon usage and different open reading frames. *Exp. Cell Res.* **298**, 431-444.
Yamamichi-Nishina, M., Ito, T., Mizutani, T., Yamamichi, N., Watanabe, H. and Iba, H. (2003). SW13 cells can transition between two distinct subtypes by switching expression of BRG1 and Brm genes at the post-transcriptional level. *J. Biol. Chem*. **278**, 7422-7430.